

Detection and Visualization of Food-derived Polyphenols by Matrix-assisted Laser Desorption/Ionization Mass Spectrometry Imaging

Huu-Nghi Nguyen,¹ Tae Hun Ham,² Toshiro Matsui,^{2,3} and Mitsuru Tanaka^{2,3*}

¹Faculty of Biotechnology and Food Technology, Thai Nguyen University of Agriculture and Forestry,
Thai Nguyen City, Vietnam

²Division of Bioscience and Bioenvironmental Sciences, Faculty of Agriculture,
Graduate School of Kyushu University, 744 Motoooka, Nishi-ku, Fukuoka 819-0395, Japan

³Research and Development Center for Five-Sense Devices, Kyushu University,
744 Motoooka, Nishi-ku, Fukuoka 819-0395, Japan

(Received March 14, 2019; accepted May 14, 2019)

Keywords: MALDI-MS, polyphenols, visualization

Food-derived polyphenols have health benefits owing to their ability to prevent some diseases. Knowledge of their bioavailabilities and metabolism is important for understanding the mechanisms underlying their benefits. Thus, mass spectrometry (MS)-based analytical techniques, such as liquid chromatography-MS (LC-MS), that are capable of highly sensitive and simultaneous detection of absorbed polyphenols and their metabolites are essential tools in this field. Matrix-assisted laser desorption/ionization mass spectrometry (MALDI-MS) imaging is currently used in biological sciences for visualizing the spatial information of various compounds, such as peptides, proteins, lipids, drugs, and food compounds, in various biological tissues. However, the application of MALDI-MS imaging to polyphenols is challenging owing to the lack of appropriate matrix reagents for visualizing (or detecting) polyphenols absorbed in target biological tissues. This review highlights the development of the MALDI-MS imaging technique for the detection and visualization of food-derived polyphenols. First, the development of new matrices and matrix additives for the detection and visualization of polyphenols is discussed, followed by their introduction to inhibitor-aided MALDI-MS imaging for the elucidation of intestinal absorption routes and the metabolic behaviors of polyphenols. The MALDI-MS imaging technique shows great potential as a novel analytical tool for elucidating the bioavailabilities of food-derived polyphenols.

1. Introduction

Food-derived polyphenols, which occur naturally in tea, coffee, and a wide variety of fruits and vegetables, are consumed worldwide owing to their potential health benefits, such as the prevention of cardiovascular diseases,^(1,2) diabetes,⁽³⁾ and cancers,^(4,5) as well as intestinal regulation for the absorption of other compounds.⁽⁶⁾ To understand the mechanisms underlying

*Corresponding author: e-mail: mitsurut@agr.kyushu-u.ac.jp
<https://doi.org/10.18494/SAM.2019.2371>

their bioactivities, their absorption, distribution, metabolism, and excretion (ADME) behaviors must be elucidated. Owing to their complex absorption behaviors and metabolic processes, such as methylation, sulfation, and glucuronidation,^(7–9) mass spectrometry (MS)-based analytical techniques such as liquid chromatography-MS (LC-MS) techniques with high sensitivity and throughput characteristics are considered useful.^(10–13) However, despite their widespread application, LC-based methods present several drawbacks in terms of laborious pretreatment processes, such as preparation and extraction steps, which can lead to loss of information regarding the localization of analytes in biological tissues.⁽¹⁴⁾ Matrix-assisted laser desorption/ionization mass spectrometry (MALDI-MS) is widely used for the simultaneous detection of both low- and high-molecular-weight target compounds without the aforementioned pretreatment processes owing to its advantages in terms of sensitivity, selectivity, and tolerance to impurities.^(15,16) Accordingly, MALDI-MS is used to detect a diverse range of ionizable compounds, such as proteins, lipids, and drug molecules.^(17–19) Currently, the development of MALDI-MS-aided imaging is receiving considerable attention since it not only provides information on the presence of compounds, but can also be used to visualize their distribution and/or localization in biological tissues, overcoming the limitations of LC-MS methods.^(14,20,21) The combination of MS detection with spatial localization presents a novel scientific methodology for food and drug development fields.^(14,22) Numerous reports on the application of MALDI-MS imaging to the visualization of a wide mass range of peptides,⁽²³⁾ proteins,^(24,25) lipids,⁽²⁶⁾ drugs,^(27–29) and food compounds⁽³⁰⁾ have been published. However, the application of MALDI-MS imaging to the visualization of polyphenols is challenging owing to the lack of appropriate matrix reagents for detecting and/or visualizing target polyphenols with low bioavailabilities. Therefore, the present review focuses on the development of MALDI-MS as a technique for detecting and visualizing food-derived polyphenols in biological tissues. This novel MS imaging technique provides a powerful analytical strategy for understanding the ADME behaviors of polyphenols.

2. MALDI-MS Imaging Principle

The general procedure for MALDI-MS imaging is illustrated in Fig. 1. Typically, it comprises tissue preparation, matrix application, and MS imaging data acquisition, followed by data analysis and image construction. The sample, which may be any type of biological tissue, is cryosectioned into slices with μm thicknesses, which are then mounted onto indium-tin oxide (ITO)-coated conductive glass slides. The mounted slices are then coated with a MALDI matrix to extract the analytes from the tissue surface into a matrix crystal and to aid desorption/ionization in the mass spectrometer. Upon irradiation by a UV laser, the matrix absorbs the laser energy and transforms the analytes into the gas phase, promoting the ionization of the analytes in the matrix plume. MALDI sources are equipped with a UV laser, such as a nitrogen laser (337 nm) or a Nd-YAG laser (355 nm).⁽³¹⁾ The MALDI technique is usually combined with time-of-flight (TOF)-MS or high-resolution MS such as Fourier-transform ion cyclotron resonance (FT-ICR)-MS.⁽³²⁾ Mass spectra are acquired from defined geometrical coordinates across the tissue. The analytes are detected on the basis of m/z (a

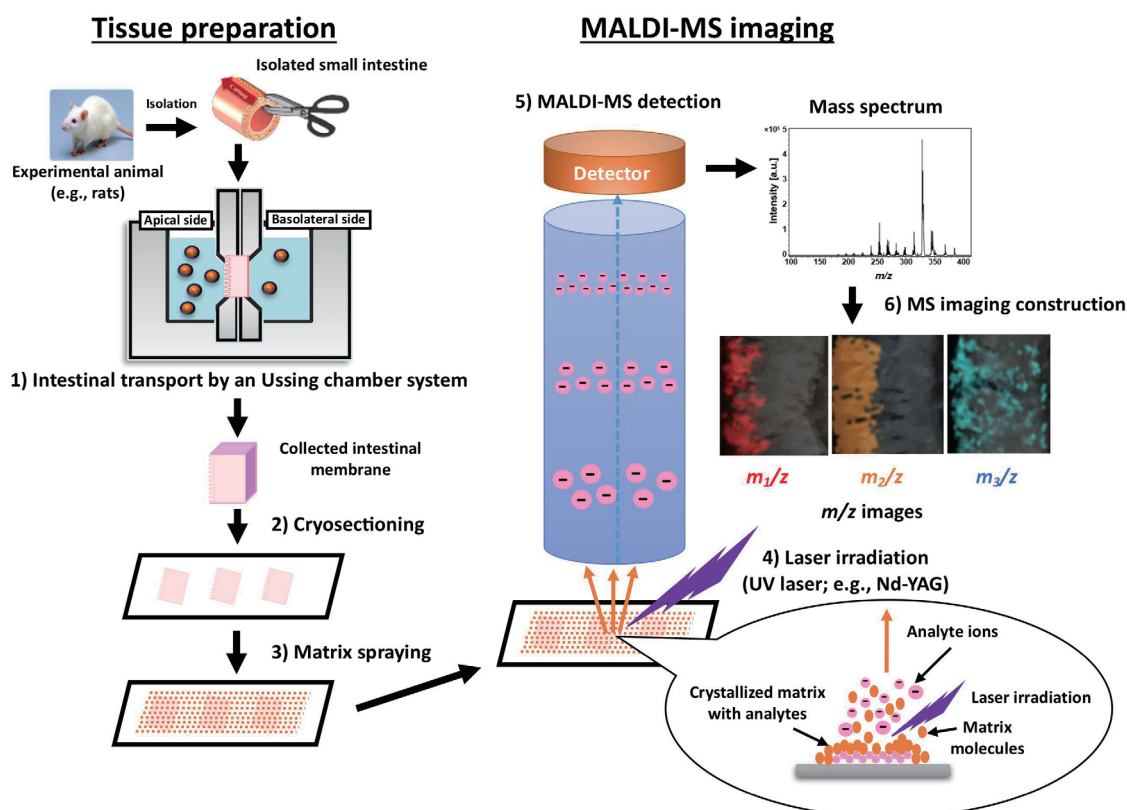


Fig. 1. (Color online) General workflow of MALDI-MS imaging for visualization of polyphenols after intestinal transport experiment using an Ussing chamber system. 1) Intestinal transport by Ussing chamber system: the rat small intestine is isolated and cut along the mesenteric border to expose the mucosal side and subsequently mounted on the Ussing chamber system. The polyphenol sample is added to the apical compartment to transport it across the intestinal membrane. 2) Cryosectioning: the intestinal membrane after the transport was collected and then cryosectioned into slices with μm thickness. The slices are thaw-mounted on ITO-coated slide glass. 3) Matrix spraying: tissue slices on ITO glass slides are homogeneously spray-coated with an appropriate matrix. 4) Laser irradiation: the matrix-coated slices are inserted into the MALDI-MS instrument and irradiated using a UV laser to ionize analytes. 5) MALDI-MS detection: the analytes are detected on the basis of their mass-to-charge ratios (m/z values) in generated mass spectra. 6) MS imaging construction: a custom software program is used to compile the mass spectra into a format where intensities of all detected analytes can be visualized across the tissue as ion density images.

dimensionless quantity obtained by dividing the ratio of the mass of an ion to the unified atomic mass unit, by its charge number⁽³³⁾ in the generated mass spectra. Custom software is used to compile the mass spectra into a certain image format in which the presence of the analytes detected can be visualized across the tissue as ion density images.⁽³⁴⁾ MALDI-MS imaging is typically performed at spatial resolutions of 10 to 200 μm .⁽³²⁾ The pseudo-color images thus obtained allow the visualization of the distributions of molecules of interest in biological tissues to be visualized.

3. MALDI-MS Imaging for Polyphenol Analysis

3.1 Matrix selection for MALDI-MS visualization of polyphenols

Matrix selection is critical for analyte detection by MALDI-MS. In general, matrix reagents for MALDI must exhibit a strong absorption at the laser irradiation wavelength used, good compatibility between the analytes and the matrix solvent, good vacuum stability, a low vapor pressure, and the ability to participate in protonation or deprotonation reactions in the gas phase.⁽¹⁶⁾ Matrix reagents for a negative MALDI mode should be strong bases in order to abstract a proton from analytes, whereas a high acidity in the gas phase that donates a proton to analytes appears to be an important characteristic of matrices for a positive MALDI mode.⁽³⁵⁾ Matrices such as α -cyano-4-hydroxycinnamic acid (CHCA), sinapinic acid (SA), and 2,5-dihydroxybenzoic acid (DHB) have been widely used in the positive-charge MALDI detection of proteins, peptides, and lipids owing to the positively charged characteristics of their nitrogen-containing chemical structures.⁽³⁶⁾ However, the MALDI-MS detection of polyphenols, which have neutral chemical structures (except for anthocyanins, which have positively charged flavylum skeletons), has severe limitations owing to their lack of proton removal or addition groups.⁽³⁷⁾ Moreover, there are several limitations for the aforementioned conventional matrices, such as an abundance of interfering signals in the low-mass range for a positive detection mode and a low ionization efficiency for a negative detection mode.⁽³⁶⁾

Several attempts at detecting polyphenols by MALDI-MS have been reported in the literature, as listed in Table 1. One strategy for the MALDI-MS detection of polyphenols is to monitor them as metal adducts. For instance, theaflavins and hesperidin were detected as $[M+Na]^+$ and $[M+K]^+$ adducts in positive-mode MALDI-MS using conventional CHCA and DHB matrices, respectively.^(15,38) The detection of proanthocyanidins as $[M+Cs]^+$ and $[M+Ag]^+$ has also been reported.⁽¹⁶⁾ Another strategy is to use basic matrices such as *trans*-3-indoleacrylic acid (IAA)⁽³⁹⁾ and 1,5-diaminonaphthalene (1,5-DAN)⁽³⁰⁾ in the negative MS detection mode. Since basic matrices abstract a proton from analytes, these matrices have been used to detect proanthocyanidins and epigallocatechin gallate (EGCG) as $[M-H]^-$.^(30,39) The photobase generator nifedipine (λ_{max} at 344 nm)⁽⁴⁰⁾ has recently been developed as a unique MALDI matrix reagent that can deprotonate polyphenols because the photobase produced from nifedipine can act as a catalyst in UV-mediated polymer cross-linking reactions owing to its proton abstracting ability.^(41,42) A variety of polyphenols including flavonols, flavones, flavanones, flavonones, chalcones, stilbenoids, and phenolic acids were successfully detected as $[M-H]^-$ by nifedipine-aided MALDI-MS in the negative mode with markedly higher intensities than those reported for other matrices such as IAA [Fig. 2(a)].⁽³⁷⁾ The mechanism of nifedipine-induced MS ionization of polyphenols involves the production of a nitrosophenyl pyridine derivative from nifedipine under laser irradiation at 355 nm.⁽³⁷⁾ This photobase product plays a crucial role in the deprotonation of polyphenols in negative-mode MALDI-MS [as illustrated in Fig. 2(b)].⁽³⁷⁾ Moreover, the enhanced detection of polyphenols was achieved by the addition of phytic acid, which has been reported as a matrix additive for enhancing the MALDI-MS detection of peptides.⁽⁴³⁾ According to the nifedipine-aided MALDI-MS analysis

Table 1
Matrices for MALDI-MS detection of polyphenols.

Matrix	Structure	Detection mode	Analyte	Detected ion type	Reference
DHB		Positive	Epicatechin Epigallocatechin Afzelechin Fisetinidol Robinetinidol	$[M+Na]^+$ $[M+K]^+$	16
			Cyanidin pentoside Cyanidin hexoside Cyanidin dihexoside	$[M]^+$	44
CHCA		Positive	Hesperidin	$[M+Na]^+$	37
		Negative	Theaflavin; Theaflavin-3-gallate Theaflavin-3'-gallate Theaflavin-3, 3'-digallate Theaflavate A Theaflavate B	$[M+H]^+$ $[M+Na]^+$ $[M+K]^+$	15
IAA		Negative	Quercetin hexoside Kaempferol hexoside Phloretin hexoside	$[M-H]^-$	43
			Catechin (dimer and oligomer)	$[M-H]^-$	38
1,5-DAN		Negative	Epigallocatechin gallate	$[M-H]^-$	30
Nifedipine		Negative	Epigallocatechin gallate Theaflavin-3'-gallate Epicatechin Epicatechin gallate Theasinensin A Procyanidin B2 Luteolin Acacetin Naringenin Naringin Hesperidin Kaempferol Quercetin Curcumin Resveratrol Ellagic acid	$[M-H]^-$	36, 52
			Matrix free	—	Negative and positive

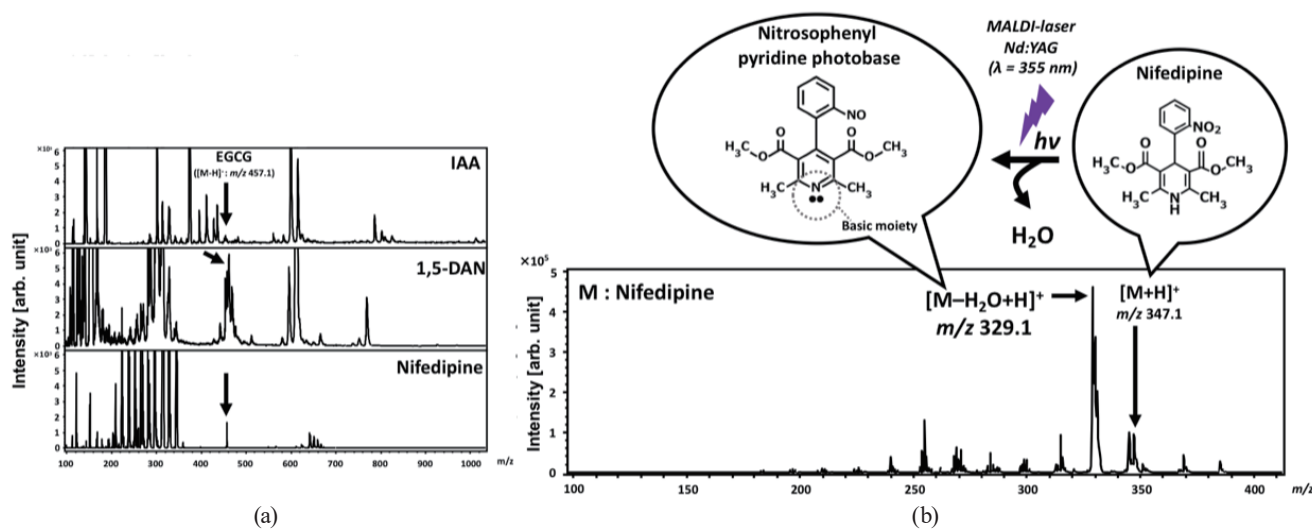


Fig. 2. (Color online) (a) MALDI-MS detection of EGCG (1 pmol/spot) using IAA, 1,5-DAN, and a photobase generator, nifedipine, in negative mode. (b) Generation and detection of a MALDI-laser-induced photobase, nitrosophenyl pyridine, by MALDI-MS analysis of nifedipine in positive mode.

of methylated naringenins, the OH group at the 5-position of the flavonoid skeleton A-ring undergoes proton removal by nifedipine.⁽³⁷⁾ Thus, nifedipine may be useful as a novel and powerful MALDI matrix reagent for the analysis of polyphenols and may contribute to the future application of MALDI-MS imaging for investigating the bioavailability of bioactive polyphenols.

3.2 Visualization of polyphenol distributions in edible plants by MALDI-MS imaging

Polyphenols are plant metabolites during growth and development. Thus, understanding the distribution of polyphenols in plant tissues is important for elucidating the biological processes that occur in plants. MALDI-MS imaging has been used to visualize the distribution of flavonoid glycosides in apple.⁽⁴⁴⁾ In that study, the different distribution behaviors of flavonoid glycosides such as quercetin hexoside, kaempferol hexoside, and phloretin hexoside in the skin region and in the pericarp were determined.⁽⁴⁴⁾ The localization of anthocyanins such as cyanidin pentoside, cyanidin hexoside, and cyanidin dihexoside in black rice has been investigated by MALDI-MS imaging, revealing that anthocyanins composed of different sugar moieties exhibit different localization patterns in the pericarp of black rice.⁽⁴⁵⁾ MALDI-MS imaging has also revealed that, unlike other flavonoids, vicenin-2 is produced at the top of *Lychnophora salicifolia* leaves.⁽⁴⁶⁾ The combination of the localization and UV absorption properties of vicenin-2 indicate that it could act as a UV-light barrier to protect plants. Thus, MALDI-MS imaging provides information vital for understanding the ecological and physiological functions of metabolites in plants.⁽⁴⁶⁾ The presence of hesperidin in leaves and stems of *Citrus limonia* after *Xylella fastidiosa* infection has been visualized by MALDI-MS imaging, revealing that hesperidin plays a role in the plant-pathogen interaction.⁽³⁸⁾ Thus, MALDI-MS imaging could overcome the limitations of conventional analytical methods in research into the distribution of polyphenols in plant tissues, providing new analytical information regarding the biological roles and biosynthesis of phytochemicals in plants.

3.3 MALDI-MS imaging as a novel method for *in situ* visualization of polyphenol absorption in rat small intestine

MALDI-MS imaging has been widely used in drug discovery and development studies to visualize the absorption and distribution of administered drugs. The intestinal absorption behaviors of propranolol and metoprolol (high-permeability compounds) and atenolol (a low-permeability compound) were evaluated by MALDI-MS imaging.⁽²⁰⁾ The results provided novel insight into site-specific absorption along the crypt–villus axis for each of the compounds, and confirmed a proximal-distal absorption gradient along the intestine.⁽²⁰⁾ In a tuberculosis research study, several anti-tuberculosis drugs including rifampicin, pyrazinamide, and moxifloxacin were administered to patients, and MALDI-MS imaging was used to visualize the distribution of these drugs in tuberculosis lesions.⁽²⁷⁾ The results revealed that rifampicin and pyrazinamide efficiently penetrated the tuberculosis infection sites in lung lesions but did not diffuse well in caseum.⁽²⁷⁾ However, the MALDI-MS imaging of polyphenols distributed in biological tissue is limited owing to their low bioavailabilities. There is only one report on the application of MALDI-MS imaging to the visualization of polyphenols administered in biological tissues. In that study, Kim *et al.* achieved the *in situ* visualization of EGCG in rat liver and kidney after the administration of a 2000 mg EGCG/kg rat body weight dose,⁽³⁰⁾ demonstrating that MALDI-MS imaging may be applicable to the evaluation of the bioavailability of polyphenols.

It has been reported that the small intestine is the organ mainly responsible for the absorption of polyphenols with low bioavailabilities.⁽⁴⁷⁾ Therefore, evaluating the intestinal absorption and metabolism of polyphenols is important for understanding their bioavailability and mechanism of absorption. Although a cell-based *in vitro* intestinal epithelial model using Caco-2 cells is commonly used,^(48,49) the Caco-2 cell model exhibits several shortcomings, such as differences in protease expression from those in actual intestinal membranes. An *ex vivo* animal intestinal membrane mounted on an Ussing chamber system is a promising alternative and has been used to investigate the transport of drugs and food compounds.^(23,50,51) Enhanced MALDI-MS imaging using nifedipine with phytic acid was used to visualize the accumulation of an absorbable epicatechin gallate (ECG)⁽⁵²⁾ in the rat small intestinal membrane after an Ussing chamber transport experiment, revealing that ECG was distributed throughout the entire jejunum membrane [Fig. 3(c)].⁽⁵³⁾ The involvement of intestinal membrane uptake transporters such as monocarboxylic transporter (MCT) and organic anion-transporting polypeptide (OATP) in the cellular uptake of polyphenols has been reported.^(48,54–56) Therefore, the elucidation of intestinal absorption routes for polyphenols is important. Accordingly, MALDI-MS imaging has been applied to investigating the intestinal transport of these polyphenols with the aid of transporter inhibitors. To elucidate the possible absorption route(s) of polyphenols, phloretin (an MCT inhibitor),⁽⁵⁷⁾ estrone-3-sulfate (an OATP inhibitor),⁽⁵⁵⁾ and wortmannin (a transcytosis inhibitor)⁽⁵⁸⁾ have been used in intestinal ECG transport experiments.⁽⁵³⁾ The significant reduction in the level of ECG distribution in the intestinal membrane in the presence of phloretin and estrone-3-sulfate clearly demonstrated the involvement of MCT and OATP in the intestinal transport of ECG, respectively [Fig. 4(a)], was reported by Vaidyanathan and Walle.⁽⁴⁸⁾

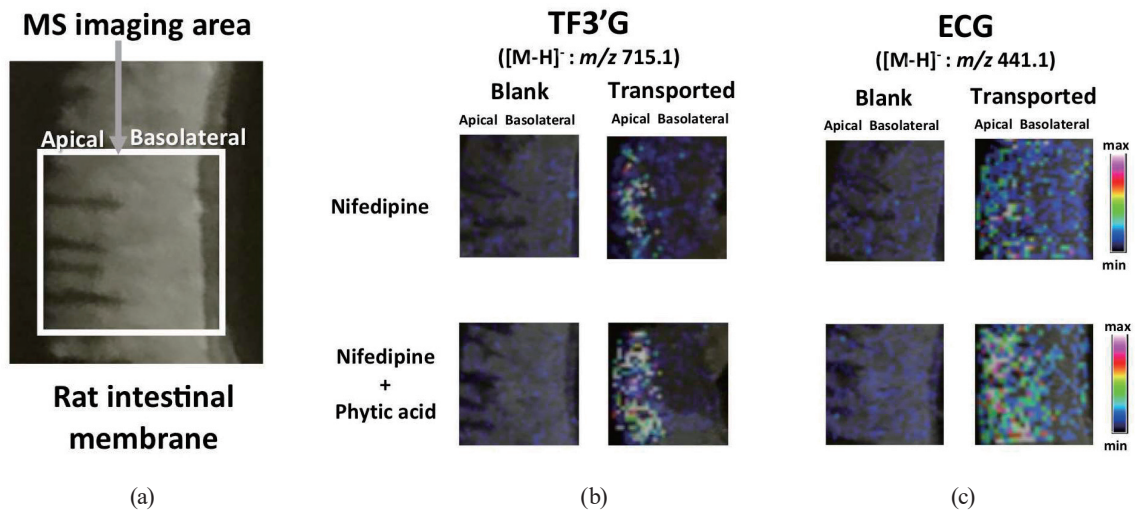


Fig. 3. (Color online) Nifedipine-aided MALDI-MS imaging of TF3'G and ECG in intestinal tissues after Ussing chamber transport experiments and enhanced MALDI-MS detection of polyphenols. (a) Representative optical image of the rat jejunum membrane and distributions of (b) TF3'G, and (c) ECG in the membranes.

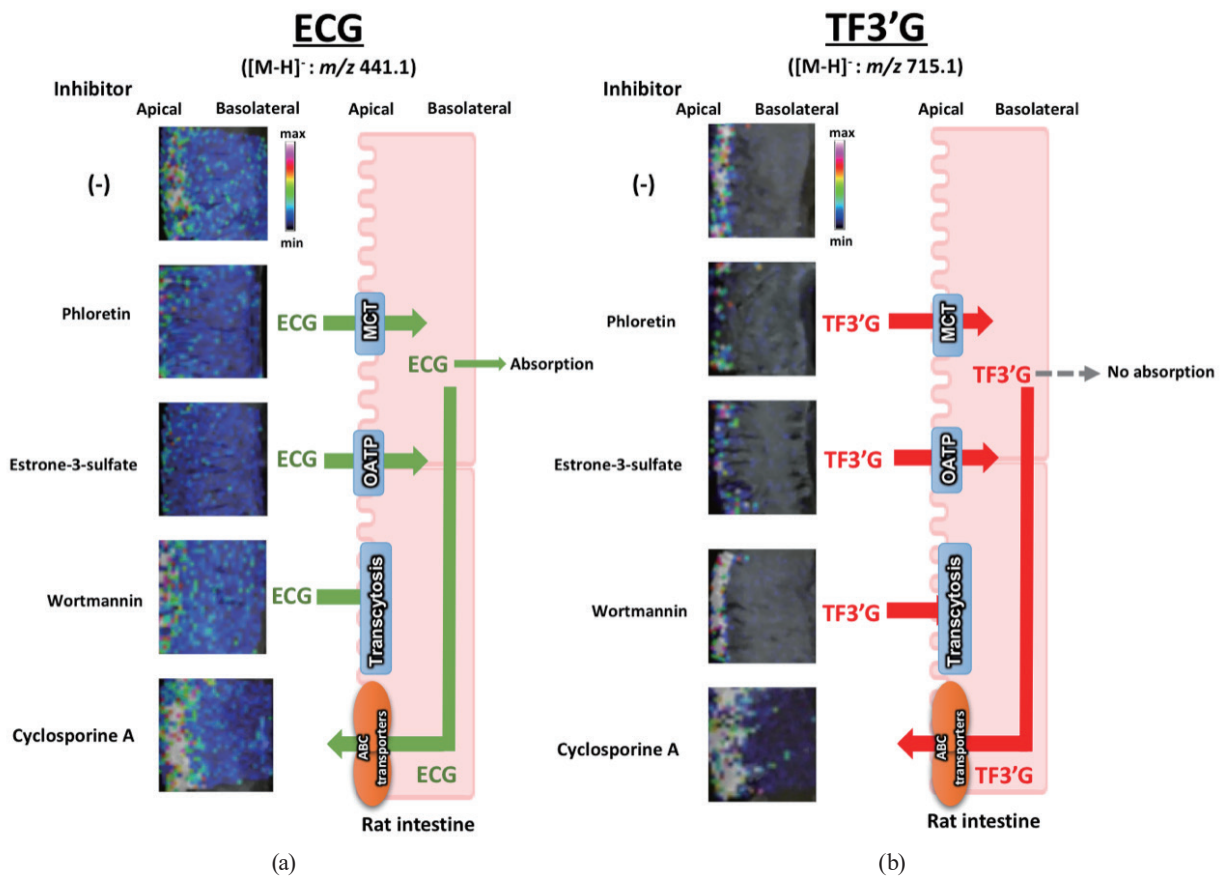


Fig. 4. (Color online) *In situ* visualization of intestinal absorption processes of (a) ECG and (b) TF3'G by nifedipine-aided MALDI-MS imaging. MCT: monocarboxylic transporter, OATP: organic anion transporting polypeptide, and ABC transporters: ATP-binding cassette efflux transporters.

Moreover, the *in situ* MALDI-MS imaging of the intestinal membrane has also been applied to the evaluation of the involvement of efflux ABC transporters, including multidrug resistance protein 2 (MRP2), P-glycoprotein (P-gp), and breast cancer resistance protein (BCRP),⁽⁵⁹⁾ since the low bioavailability of polyphenols is considered to be partly due to their intestinal efflux.⁽⁶⁰⁾ The cotransport of cyclosporine A [a nonspecific ATP-binding cassette (ABC) efflux transport inhibitor] and ECG provided a marked increase in visualized intensity localized on the apical side of the intestinal membrane,⁽⁶¹⁾ clearly illustrating the involvement of ABC transporters in the transport of ECG [Fig. 4(a)]. Thus, the inhibitor-aided MALDI-MS imaging technique is a powerful and novel analytical tool for the direct analysis of the intestinal absorption of analytes without the pretreatment steps, such as extraction and separation, required in LC and LC-MS analyses.⁽⁵³⁾

Inhibitor-aided intestinal MALDI-MS imaging has also been used to investigate the absorption of nonabsorbable theaflavin-3'-*O*-gallate (TF3'G),⁽⁴⁷⁾ which can regulate the intestinal expression of peptide transporter 1 (PepT1) and tight-junction (TJ)-related proteins (claudin-1, ZO-1, and occludin) in order to inhibit the intestinal transport of peptides and TJ-mediated substrates.^(62,63) Interestingly, although TF3'G was not absorbed, the apical-specific localization of TF3'G on an intestinal membrane after Ussing chamber transport was clearly visualized [Fig. 3(b)]. The visualized TF3'G disappeared in the presence of phloretin and estron-3-sulfate, and was enhanced by cyclosporine A [Fig. 4(b)].⁽⁵³⁾ Thus, these visualized results demonstrated for the first time that TF3'G can be incorporated into intestinal tissues through MCT or OATP followed by efflux back to the apical compartment, and this discovery will help elucidate the mechanism of the regulatory effect of TF3'G on the expression of PepT1 and TJ proteins. Such observation of tissue incorporation of nonabsorbable polyphenols is due to the great advantage of *in situ* tissue visualization by MALDI-MS imaging, which indicates the potential use of the present MS imaging technique for the elucidation of intestinal transport mechanisms of substrates including absorbable and nonabsorbable polyphenols.

3.4 Visualization of polyphenol metabolites in rat small intestine by MALDI-MS imaging

Understanding metabolic behaviors (endogenous and exogenous metabolisms) is essential for obtaining insights into the mechanisms of molecular changes associated with physiological alterations, such as those induced by diseases and aging, and for evaluating the bioavailabilities of drugs and food compounds upon oral administration. MALDI-MS imaging has also been used to visualize a broad range of endogenous metabolites (e.g., nucleotides, cofactors, phosphorylated sugars, amino acids, lipids, and carboxylic acids in brain tissues)⁽⁶⁴⁾ and drugs/drug metabolites after oral administration (e.g., terfenadine and its metabolites, fexofenadine in the small intestine and liver,⁽²⁸⁾ and erlotinib and its demethylated conjugates localized at tumor areas in the lung⁽⁶⁵⁾). According to previous reports demonstrating that polyphenols undergo a complex phase-II metabolism including methylation, sulfation, and glucuronidation upon oral administration,^(8,66) the low bioavailability of polyphenols is due to not only their poor absorption but also their extensive metabolism. A lot of research has been

dedicated to identifying phase-II metabolites of polyphenols in plasma and tissues using LC-MS methods.^(7,67–69) However, detailed information on the localization of these metabolites in organs remains unclear.⁽³¹⁾ Exploiting the advantages of MALDI-MS imaging for the nontargeting analysis of compounds, the nifedipine-aided MALDI-MS visualization technique was applied to the elucidation of the metabolic behavior of TF3'G and ECG during their intestinal absorption. Interestingly, MALDI-MS imaging successfully visualized the phase-II metabolites of ECG, including their sulfated, methylated, and methyl-sulfated forms [Fig. 5(a)], as had been observed in plasma after oral administration to Wistar rats,⁽⁶⁹⁾ Caco-2 cell monolayers,⁽⁴⁹⁾ and the human intestine.⁽⁷⁰⁾ In time-course transport experiments, sulfate ECG was visualized after 15 min transport in the intestinal membrane prior to the formation of methylated- and methyl-sulfated conjugates (30–60 min transport). Conversely, phase-II metabolites of TF3'G were not detected in the study [Fig. 5(b)].⁽⁵³⁾ Considering the results of a previous study in which TFs and their phase-II metabolites were not detected in human urine after the oral administration of 1000 mg TF extract, TFs seem to be stable against phase-II

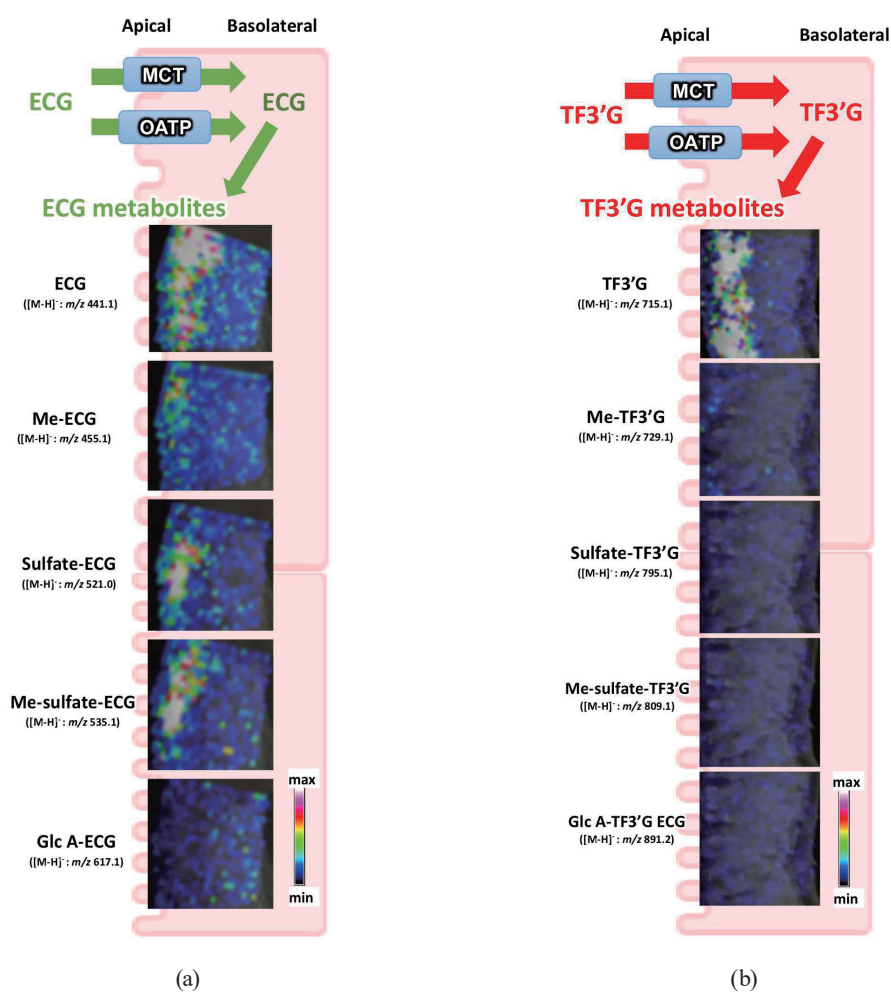


Fig. 5. (Color online) Simultaneous visualization of phase-II metabolites of (a) ECG and (b) TF3'G in intestine by nifedipine-aided MALDI-MS imaging. Me: methylated and Glc A: glucuronidated.

metabolism in the intestinal tissue.⁽⁷¹⁾ Moreover, MALDI-MS imaging has also been applied in the *in vivo* study of polyphenol metabolism, in which sulfate and glucuronide metabolites of EGCG were visualized in liver and kidney tissues after its oral administration.⁽³⁰⁾ Thus, the simultaneous visualization of various polyphenol metabolites may be used to investigate the complex phase-II metabolism of polyphenols in the intestine and liver.

4. Conclusions and Future Challenges

The MALDI-MS imaging technique has been developed as a means to elucidate the bioavailability of polyphenols, their absorption mechanisms, and their metabolic behavior in the intestine. The *in situ* tissue visualization of small substrates such as polyphenols by MS imaging is extremely useful for acquiring the spatial information required to elucidate their biological roles in plants and animal organs. Clearly, this spatial information cannot be obtained by immunohistochemistry approaches or other MS-based techniques (such as LC-MS). However, the MALDI-MS technique seems to be unsuitable for quantitative analysis owing to the poor reproducibility (both sample-to-sample and shot-to-shot) caused by inhomogeneous matrix crystal formation, interference from concomitant compounds, and the destruction of analytes by laser shots.⁽⁷²⁾ According to recently published research by Nakamura *et al.*⁽⁷³⁾ regarding the MALDI-MS detection of plasma amyloid- β biomarkers for Alzheimer's disease, the use of appropriate internal standards (i.e., stable-isotope-labeled analytes or their analogues) is a viable strategy for overcoming this disadvantage. Thus, in the view of the aforementioned (and potential future) development of MALDI-MS imaging, this *in situ* technique may serve as a powerful and novel analytical tool for investigating the absorption and metabolism of polyphenols.

Acknowledgments

This work was supported in part by a grant-in-aid from the Ministry of Education, Science, Sports, and Culture of Japan (No. 18K05534 to M. T. and No. 18H02157 to T. M.), and in part by a grant-in-aid from the Tojuro Iijima Foundation for Food Science and Technology to M. T. The authors thank Ms. Kaori Miyazaki for her technical assistance.

References

- 1 V. Stangl, M. Lorenz, and K. Stangl: *Mol. Nutr. Food Res.* **50** (2006) 218. <https://doi.org/10.1002/mnfr.200500118>
- 2 H. Pan, Y. Gao, and Y. Tu: *Molecules* **21** (2016) 1659. <https://doi.org/10.3390/molecules21121659>
- 3 M. C. Sabu, K. Smitha, and R. Kuttan: *J. Ethnopharmacol.* **83** (2002) 109. [https://doi.org/10.1016/S0378-8741\(02\)00217-9](https://doi.org/10.1016/S0378-8741(02)00217-9)
- 4 C. S. Yang and H. Wang: *Molecules* **21** (2016) 1679. <https://doi.org/10.3390/molecules21121679>
- 5 C. S. Yang, X. Wang, G. Lu, and S. C. Picinich: *Nat. Rev. Cancer* **9** (2009) 429. <https://doi.org/10.1038/nrc2641>
- 6 M. Shimizu, Y. Kobayashi, M. Suzuki, H. Satsu, and Y. Miyamoto: *BioFactors* **13** (2000) 61. <https://doi.org/10.1002/biof.5520130111>
- 7 M. Margalef, Z. Pons, F. I. Bravo, B. Muguerza, and A. Arola-Arnal: *J. Nutr. Biochem.* **26** (2015) 987. <https://doi.org/10.1016/j.jnutbio.2015.04.006>

- 8 S. Sang, J. D. Lambert, C. T. Ho, and C. S. Yang: *Pharmacol. Res.* **64** (2011) 87. <https://doi.org/10.1016/j.phrs.2011.02.007>
- 9 A. Stalmach, S. Troufflard, M. Serafini, and A. Crozier: *Mol. Nutr. Food Res.* **53** (2009) S44. <https://doi.org/10.1002/mnfr.200800169>
- 10 T. P. J. Mulder, C. J. van Platerink, P. J. Wijnand Schuyl, and J. M. M. van Amelsvoort: *J. Chromatogr. B* **760** (2001) 271. [https://doi.org/10.1016/S0378-4347\(01\)00285-7](https://doi.org/10.1016/S0378-4347(01)00285-7)
- 11 M. J. Motilva, A. Serra, and A. Macià: *J. Chromatogr. A* **1292** (2013) 66. <https://doi.org/10.1016/j.chroma.2013.01.012>
- 12 R. K. Bonta: *J. Pharm. Anal.* **7** (2017) 349. <https://doi.org/10.1016/j.jpba.2017.06.005>
- 13 W. Pongsuwan, T. Bamba, K. Harada, T. Yonetani, A. Kobayashi, and E. Fukusaki: *J. Agric. Food Chem.* **56** (2008) 10705. <https://doi.org/10.1021/jf8018003>
- 14 A. R. Buchberger, K. DeLaney, J. Johnson, and L. Li: *Anal. Chem.* **90** (2018) 240. <https://doi.org/10.1021/acs.analchem.7b04733>
- 15 M. C. Menet, S. Sang, C. S. Yang, C. T. Ho, and R. T. Rosen: *J. Agric. Food Chem.* **52** (2004) 2455. <https://doi.org/10.1021/jf035427e>
- 16 M. Monagas, J. E. Quintanilla-López, C. Gómez-Cordovés, B. Bartolomé, and R. Lebrón-Aguilar: *J. Pharm. Biomed. Anal.* **51** (2010) 358. <https://doi.org/10.1016/j.jpba.2009.03.035>
- 17 P. Millares, E. J. LaCourse, S. Perally, D. A. Ward, M. C. Prescott, J. E. Hodgkinson, P. M. Brophy, and H. H. Rees: *PLoS One* **7** (2012) e33590. <https://doi.org/10.1371/journal.pone.0033590>
- 18 L. Li, J. Han, Z. Wang, J. Liu, J. Wei, S. Xiong, and Z. Zhao: *Int. J. Mol. Sci.* **15** (2014) 10492. <https://doi.org/10.3390/ijms150610492>
- 19 A. K. Su, J. T. Liu, and C. H. Lin: *Talanta* **67** (2005) 718. <https://doi.org/10.1016/j.talanta.2005.03.013>
- 20 A. Nilsson, A. Peric, M. Strimfors, R. J. A. Goodwin, M. A. Hayes, P. E. Andrés, and C. Hilgendorf: *Sci. Rep.* **7** (2017) 6352. <https://doi.org/10.1038/s41598-017-06583-4>
- 21 K. Schwamborn and R. M. Caprioli: *Mol. Oncol.* **4** (2010) 529. <https://doi.org/10.1016/j.molonc.2010.09.002>
- 22 A. Nilsson, R. J. A. Goodwin, M. Shariatgorji, T. Vallianatou, P. J. H. Webborn, and P. E. Andrés: *Anal. Chem.* **87** (2015) 1437. <https://doi.org/10.1021/ac504734s>
- 23 M. Tanaka, S. M. Hong, S. Akiyama, Q. Q. Hu, and T. Matsui: *Mol. Nutr. Food Res.* **59** (2015) 1541. <https://doi.org/10.1002/mnfr.201500075>
- 24 M. W. Duncan, D. Nedelkov, R. Walsh, and S. J. Hattan: *Clin. Chem.* **62** (2016) 134. <https://doi.org/10.1373/clinchem.2015.239491>
- 25 M. Dilillo, R. Ait-Belkacem, C. Esteve, D. Pellegrini, S. Nicolardi, M. Costa, E. Vannini, E. L. De Graaf, M. Caleo, and L. A. McDonnell: *Sci. Rep.* **7** (2017) 603. <https://doi.org/10.1038/s41598-017-00703-w>
- 26 X. Wang, J. Han, A. Chou, J. Yang, J. Pan, and C. H. Borchers: *Anal. Chem.* **85** (2013) 7566. <https://doi.org/10.1021/ac401595a>
- 27 B. Prideaux, L. E. Via, M. D. Zimmerman, S. Eum, J. Sarathy, P. O'Brien, C. Chen, F. Kaya, D. M. Weiner, P. Y. Chen, T. Song, M. Lee, T. S. Shim, J. S. Cho, W. Kim, S. N. Cho, K. N. Olivier, C. E. Barry, and V. Dartois: *Nat. Med.* **21** (2015) 1223. <https://doi.org/10.1038/nm.3937>
- 28 J. Chen, Y. Hsieh, I. Knemeyer, L. Crossman, and W. A. Korfmacher: *Drug Metab. Lett.* **2** (2008) 1. <https://doi.org/10.2174/187231208783478461>
- 29 B. Spengler: *Anal. Chem.* **87** (2015) 64. https://doi.org/10.1007/978-1-4939-1357-2_5
- 30 Y. H. Kim, Y. Fujimura, T. Hagihara, M. Sasaki, D. Yukihira, T. Nagao, D. Miura, S. Yamaguchi, K. Saito, H. Tanaka, H. Wariishi, K. Yamada, and H. Tachibana: *Sci. Rep.* **3** (2013) 2805. <https://doi.org/10.1038/srep02805>
- 31 Y. Fujimura, D. Miura, and H. Tachibana: *Molecules* **22** (2017) 1621. <https://doi.org/10.3390/molecules22101621>
- 32 M. Aichler and A. Walch: *Lab. Invest.* **95** (2015) 422. <https://doi.org/10.1038/labinvest.2014.156>
- 33 K. K. Murray, R. K. Boyd, M. N. Eberlin, G. J. Langley, L. Li, and Y. Naito: *Pure Appl. Chem.* **85** (2013) 1515. <https://doi.org/10.1351/pac-rec-06-04-06>
- 34 S. Castellino, M. R. Groseclose, and D. Wagner: *Bioanalysis* **3** (2011) 24227. <https://doi.org/10.4155/bio.11.232>
- 35 R. Shroff, L. Rulisek, J. Doubsky, and A. Svatos: *Proc. Natl. Acad. Sci. U. S. A.* **106** (2009) 10092. <https://doi.org/10.1073/pnas.0900914106>
- 36 T. C. Baker, J. Han, and C. H. Borchers: *Curr. Opin. Biotechnol.* **43** (2017) 62. <https://doi.org/10.1016/j.copbio.2016.09.003>
- 37 H. N. Nguyen, M. Tanaka, G. Komabayashi, and T. Matsui: *J. Mass Spectrom.* **51** (2016) 938. <https://doi.org/10.1002/jms.3805>
- 38 M. S. Soares, D. F. Da Silva, M. R. Forim, M. F. Das Graças Fernandes Da Silva, J. B. Fernandes, P. C. Vieira, D. B. Silva, N. P. Lopes, S. A. De Carvalho, A. A. De Souza, and M. A. Machado: *Phytochemistry* **115** (2015) 161. <https://doi.org/10.1016/j.phytochem.2015.02.011>

- 39 M. Ohnishi-Kameyama, A. Yanagida, T. Kanda, and T. Nagata: *Rapid Commun. Mass Spectrom.* **11** (1997) 31. [https://doi.org/10.1002/\(SICI\)1097-0231\(19970115\)11:1<31::AID-RCM784>3.0.CO;2-T](https://doi.org/10.1002/(SICI)1097-0231(19970115)11:1<31::AID-RCM784>3.0.CO;2-T)
- 40 S. Onoue, N. Igarashi, Y. Yamauchi, N. Murase, Y. Zhou, T. Kojima, S. Yamada, and Y. Tsuda: *Eur. J. Pharm. Sci.* **33** (2008) 262. <https://doi.org/10.1016/j.ejps.2007.12.004>
- 41 W. Maafi and M. Maafi: *Int. J. Pharm.* **456** (2013) 153. <https://doi.org/10.1016/j.ijpharm.2013.07.075>
- 42 K. Suyama and M. Shirai: *Prog. Polym. Sci.* **34** (2009) 194. <https://doi.org/10.1016/j.progpolymsci.2008.08.005>
- 43 S. M. Hong, M. Tanaka, S. Yoshii, Y. Mine, and T. Matsui: *Anal. Chem.* **85** (2013) 10033. <https://doi.org/10.1021/ac402252j>
- 44 P. Franceschi, Y. Dong, K. Strupat, U. Vrhovsek, and F. Mattivi: *J. Exp. Bot.* **63** (2012) 1123. <https://doi.org/10.1093/jxb/err327>
- 45 Y. Yoshimura, N. Zaima, T. Moriyama, and Y. Kawamura: *PLoS One* **7** (2012) e31285. <https://doi.org/10.1371/journal.pone.0031285>
- 46 D. B. Silva, I. C. C. Turatti, D. R. Gouveia, M. Ernst, S. P. Teixeira, and N. P. Lopes: *Sci. Rep.* **4** (2014) 4309. <https://doi.org/10.1038/srep04309>
- 47 T. Matsui: *Eur. J. Pharmacol.* **765** (2015) 495. <https://doi.org/10.1016/j.ejphar.2015.09.017>
- 48 J. B. Vaidyanathan and T. Walle: *J. Pharmacol. Exp. Ther.* **307** (2003) 745. <https://doi.org/10.1124/jpet.103.054296.genesis>
- 49 L. Zhang, Y. Zheng, M. S. S. Chow, and Z. Zuo: *Int. J. Pharm.* **287** (2004) 1. <https://doi.org/10.1016/j.ijpharm.2004.08.020>
- 50 M. Miyake, T. Koga, S. Kondo, N. Yoda, C. Emoto, T. Mukai, and H. Toguchi: *Eur. J. Pharm. Sci.* **96** (2017) 373. <https://doi.org/10.1016/j.ejps.2016.10.006>
- 51 V. Rozehnal, D. Nakai, U. Hoepner, T. Fischer, E. Kamiyama, M. Takahashi, S. Yasuda, and J. Mueller: *Eur. J. Pharm. Sci.* **46** (2012) 367. <https://doi.org/10.1016/j.ejps.2012.02.025>
- 52 M. N. Clifford, J. J. van der Hooft, and A. Crozier: *Am. J. Clin. Nutr.* **98** (2013) 1619S. <https://doi.org/10.3945/ajcn.113.058958.1>
- 53 H. N. Nguyen, M. Tanaka, B. Li, T. Ueno, H. Matsuda, and T. Matsui: *Sci. Rep.* **9** (2019) 3166. <https://doi.org/10.1038/s41598-019-39405-w>
- 54 H. Glaeser, K. Bujok, I. Schmidt, M. F. Fromm, and K. Mandery: *Naunyn-Schmiedeberg's Arch. Pharmacol.* **387** (2014) 883. <https://doi.org/10.1007/s00210-014-1000-6>
- 55 A. Kondo, K. Narumi, J. Ogura, A. Sasaki, K. Yabe, T. Kobayashi, A. Furugen, M. Kobayashi, and K. Iseki: *Drug Metab. Pharmacokinet.* **32** (2017) 145. <https://doi.org/10.1016/j.dmpk.2016.11.009>
- 56 M. Roth, B. N. Timmermann, and B. Hagenbuch: *Drug Metab. Dispos.* **39** (2011) 920. <https://doi.org/10.1124/dmd.110.036640>
- 57 C. Shen, R. Chen, Z. Qian, X. Meng, T. Hu, Y. Li, Z. Chen, C. Huang, C. Hu, and J. Li: *Eur. J. Pharm. Sci.* **78** (2015) 214. <https://doi.org/10.1016/j.ejps.2015.07.022>
- 58 S. H. Hansen, A. Olsson, and J. E. Casanova: *J. Biol. Chem.* **270** (1995) 28425. <https://doi.org/10.1074/jbc.270.47.28425>
- 59 K. M. Giacomini, S. M. Huang, D. J. Tweedie, L. Z. Benet, K. L. R. Brouwer, X. Chu, A. Dahlin, R. Evers, V. Fischer, K. M. Hillgren, K. A. Hoffmaster, T. Ishikawa, D. Keppler, R. B. Kim, C. A. Lee, M. Niemi, J. W. Polli, Y. Sugiyama, P. W. Swaan, J. A. Ware, S. H. Wright, S. Wah Yee, M. J. Zamek-Gliszczynski, and L. Zhang: *Nat. Rev. Drug Discov.* **9** (2010) 215. <https://doi.org/10.1038/nrd3028>
- 60 K. Y. Chan, L. Zhang, and Z. Zuo: *J. Pharm. Pharmacol.* **59** (2007) 395. <https://doi.org/10.1211/jpp.59.3.0009>
- 61 M. Qadir, K. L. O. Loughlin, S. M. Fricke, N. A. Williamson, W. R. Greco, H. Minderman, and M. R. Baer: *Clin. Cancer Res.* **11** (2005) 2320. <https://doi.org/10.1158/1078-0432.CCR-04-1725>
- 62 J. Takeda, H. Y. Park, Y. Kunitake, K. Yoshiura, and T. Matsui: *Food Chem.* **138** (2013) 2140. <https://doi.org/10.1016/j.foodchem.2012.12.026>
- 63 H. Y. Park, Y. Kunitake, N. Hirasaki, M. Tanaka, and T. Matsui: *Biosci. Biotechnol. Biochem.* **79** (2015) 130. <https://doi.org/10.1080/09168451.2014.951027>
- 64 D. Miura, Y. Fujimura, M. Yamato, F. Hyodo, H. Utsumi, H. Tachibana, and H. Wariishi: *Anal. Chem.* **82** (2010) 9789. <https://doi.org/10.1021/ac101998z>
- 65 M. Nishidate, K. Yamamoto, C. Masuda, H. Aikawa, M. Hayashi, T. Kawanishi, and A. Hamada: *Sci. Rep.* **7** (2017) 16763. <https://doi.org/10.1038/s41598-017-17211-6>
- 66 J. B. Vaidyanathan and T. Walle: *Drug Metab. Dispos.* **30** (2002) 897. <https://doi.org/10.1124/dmd.30.8.897>
- 67 B. A. Warden, L. S. Smith, G. R. Beecher, D. A. Balentine, and B. A. Clevidence: *J. Nutr.* **131** (2001) 1731. <https://doi.org/10.1093/jn/131.6.1731>
- 68 J. L. Donovan, V. Crespy, C. Manach, C. Morand, C. Besson, A. Scalbert, and C. Rémésy: *J. Nutr.* **131** (2001) 1753. <https://doi.org/10.1093/jn/131.6.1753>

- 69 T. Kohri, M. Suzuki, and F. Nanjo: *J. Agric. Food Chem.* **51** (2003) 5561. <https://doi.org/10.1021/jf034450x>
- 70 L. Actis-Goretta, A. Lévêques, M. Rein, A. Teml, C. Schäfer, U. Hofmann, H. Li, M. Schwab, M. Eichelbaum, and G. Williamson: *Am. J. Clin. Nutr.* **98** (2013) 924. <https://doi.org/10.3945/ajcn.113.065789>
- 71 G. Pereira-Caro, J. M. Moreno-Rojas, N. Brindani, D. Del Rio, M. E. J. Lean, Y. Hara, and A. Crozier: *J. Agric. Food Chem.* **65** (2017) 5365. <https://doi.org/10.1021/acs.jafc.7b01707>
- 72 E. Szájli, T. Fehér, and K. F. Medzihradszky: *Mol. Cell. Proteomics* **7** (2008) 2410. <https://doi.org/10.1074/mcp.m800108-mcp200>
- 73 A. Nakamura, N. Kaneko, V. L. Villemagne, T. Kato, J. Doecke, V. Doré, C. Fowler, Q. X. Li, R. Martins, C. Rowe, T. Tomita, K. Matsuzaki, K. Ishii, K. Ishii, Y. Arahata, S. Iwamoto, K. Ito, K. Tanaka, C. L. Masters, and K. Yanagisawa: *Nature* **554** (2018) 249. <https://doi.org/10.1038/nature25456>